A Nonlinear PD Controller Design and Its Application to MOV Actuators

Yungdeug SON[1], Gang-Gyoo JIN[2]*

[1] Department of Mechanical Facility Control Engineering, Korea University of Technology and Education, 1600 Chungjeol-ro, Dongnam-gu, Cheonan, Chungnam, 31253, Korea
ydson@koreatech.ac.kr

[2] Division of Control and Automation Engineering, Korea Maritime and Ocean University,

727 Taejong-ro, Yeongdo-gu, Busan, 49112, Korea
ggjin@kmou.ac.kr (*Corresponding author*)

Abstract: This paper proposes a novel design method to control the opening and closing of a valve connected with a motor-operated valve actuator. In the structure of the proposed controller, a nonlinear gain is connected in series with the linear proportional-derivative controller with a first-order filter in the denominator. The nonlinear gain is described by a simple function of the error between the set-point and the measured output. The controller parameters are optimally tuned using a genetic algorithm (GA) so that a given objective function can be minimized. The stability of the closed-loop system is assessed using the Popov stability criterion. Simulation works are done to validate the effectiveness of the proposed method.

Keywords: MOV actuator, Nonlinear PD controller, Nonlinear function, Popov criterion.

1. Introduction

Valves adjust the flow of a fluid, such as air, water, oil, and gas through a pipe by opening or closing. They are essential components in all industrial facilities, including power and petrochemical plants, shipbuilding companies, and offshore plants. If a valve malfunctions, or if its operating speed is slower than the required value during an emergency, the power generation, water supply or other operations could be stopped and the system is in turn paralyzed. Due to recent automation trends, automatic valves can replace manual valves in cases that valves are frequently opened or closed or remotely operated, or are buried in the ground or in water, making it difficult for operators to access them.

All valves require a power source capable of generating drive torque (thrust or force), which may be electricity, pneumatic or hydraulic pressure. Among these, electric valves are frequently used for control a valve because they are simple to install, easy to use, and easy to control remotely from a long distance. Furthermore, electric valves are mechanically coupled with a gear train to provide high starting torque and satisfy the size and speed requirements.

In technologically advanced countries, a variety of models of motor-operated valve (MOV) have been developed and installed in power plants, petrochemical plants and so on. Most of the MOVs used in Korean industry depend on imports from the approved MOV manufacturers. Because MOVs contribute to the safety of the nuclear power plants as much as any other devices, the United States Nuclear Regulatory Commission (USNRC) strongly recommends that its function should be demonstrated empirically (USNRC, 1989; EPRI, 2015). Based on these US regulatory requirements, the Ministry of Science and Technology of Korea (MSTK) also recommends that the safety functions of MOVs should be verified through its regulatory administrative documents (MSTK, 1997).

Currently, the global MOV market is dominated by Limitorque's products with many different functions and in many sizes (Limitorque, 2019). Although it is not easy to access detailed development information because leading MOV manufacturers do not share their proprietary information, a series of studies on MOV characteristics and motor control have been conducted at manufacturing sites and research institutes, and in academic circles. Hussain, Behera & Alsammarae (1995) proposed important parameters for defining the general load profile and the ratings of alternating current (AC) motors of MOV operators to predict the actual torque size required to quickly open and close the MOV in cases of emergency. Jung, Kim & Lee (2004) constructed a testbed for a MOV stability test, and developed a basic test technique and a motor control center (MCC) diagnosis technique. Jung and Seong (2003) proposed a method of precisely estimating the MOV stem thrust, and Kang et al. (2011) addressed the problem of estimating the MOV stem friction coefficient.

Simple operations, such as switching the valve on and off, can be carried out with an on-off controller and a torque/limit switch, but various model-based control schemes have been employed to make the position variable. Ali & Al-Khawaldeh (2016) dealt with the methods of applying pole arrangement, fuzzy logic, neural network, and proportional–integral–derivative (PID) control theories to control the position of a direct current (DC) motor for robot arms. Wadhwani & Verma (2013) optimally tuned the parameters of a PID controller using evolutionary computation, and then applied them to a DC servo motor control. To control the position of a DC motor, Owayjan, Daou & Moreau (2015) applied four control techniques: PID, Commande Robuste d'Ordre Non Entier (CRONE), status feedback, and sliding mode control. Dessaint et al. (1990) examined the problem of inducing an adaptation technique and implementing it on a single-chip digital signal processing (DSP) board.

In this study, as a preliminary research for the development of a MOV actuator with linear motion, a nonlinear proportional-derivative (NPD) controller is proposed to control the stem position of a valve. In the structure of the NPD controller, a nonlinear gain is connected in series with the linear PD controller with a first-order filter. A simple nonlinear function is proposed as a nonlinear gain. The NPD controller is optimally tuned by a genetic algorithm (GA) in order to minimize a given objective function.

In order to examine the stability of the overall feedback system, this study applies the Popov stability criterion. Simulation works are executed to validate the performance of the proposed controller and to compare its performance with those of the standard PID controller tuned by two other methods.

This paper is organized as follows. In Section 2, a MOV actuator model is obtained. In Section 3, a nonlinear PD controller is introduced and its parameters are optimally tuned using a genetic algorithm. In Section 4, the stability analysis of the closed-loop control system is carried out using the Popov stability criterion. In Section 5, a set of simulation works are done to validate the effectiveness of the proposed controller. In the final section, we conclude the paper with some general remarks.

2. MOV Actuator Model

Electric driven MOV actuators basically consist of a motor, a protective circuit, a control and display device, a reduction gear, a valve connection, and a manual auxiliary hand wheel as shown in Figure 1.
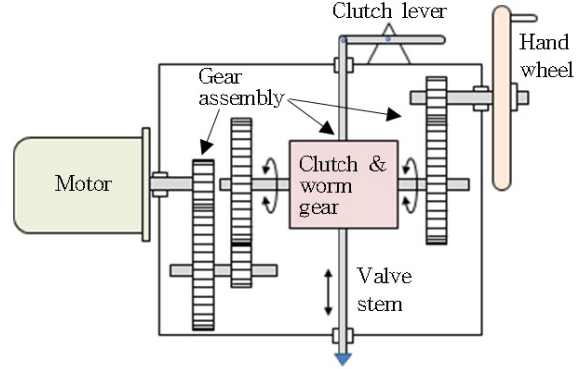

Figure 1. Architecture of a MOV actuator

In this study, as a preliminary step for developing a MOV actuator which is driven by an armature-controlled DC motor and a reduction gear, and which moves linearly, a control algorithm is obtained in order to situate the valve stem of the load size at the desired position by appropriately adjusting the input voltage of the armature circuit.

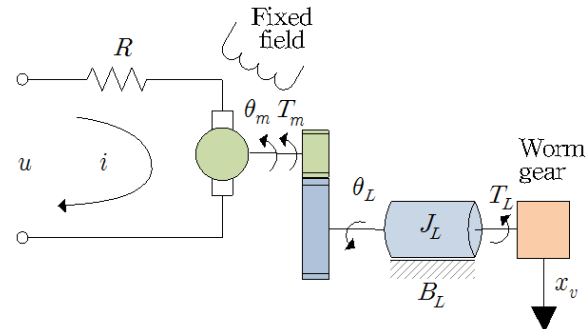The MOV actuator can be represented as an equivalent circuit as depicted in Figure 2.

Figure 2. Equivalent circuit of a MOV actuator

Assuming that the electrical time constant L/R is smaller than the mechanical time constant J_e/B_e, the model can be expressed as follows:

$$K_w u(t) - K_b \omega(t) = Ri(t) \text{,} \tag{1a}$$

$$K_t i(t) - B_e \omega(t) - T_d(t) = J_e \dot{\omega}(t) \text{,} \tag{1b}$$

$$\theta_L(t) = \frac{1}{n_g} \int \omega(t) dt \text{,} \tag{1c}$$

$$x_v(t) = K_\theta \theta_L(t) \text{,} \tag{1d}$$

where $u(t)$ is the voltage applied to the armature [V], $\omega(t)$ the angular velocity of the rotator [rad/

sec], $i(t)$ the current of the armature [A], $\theta_L(t)$ the rotation angle of the load axis [rad], $T_d(t)$ the load disturbance [N·m], $x_v(t)$ the displacement of the valve stem [mm], K_w the constant of the power converter, K_b the back electromotive force constant [V·sec], R the winding resistance of armature [Ω], K_t the torque constant [N·m/A], n_g the total gear ratio of the motor gear train, and K_θ the transfer ratio of the bevel gear train on the valve side [mm/rad].

The equivalent inertia moment J_e, the equivalent viscous friction coefficient B_e, and the load disturbance $T_d(t)$ are given by $J_e = J_m + J_L/n_g^2$, $B_e = B_m + B_L/n_g^2$, $T_d(t) = T_d(t)/n_g$, where J_m and J_L denote the inertia moments of the motor and load sides [N·m·sec²], respectively, B_m and B_L the viscous friction of the motor and load sides [N·m·sec], respectively, and T_L the torque of the load side [N·m].

The model of Equation (1) incorporating a feedback sensor can be represented by the block diagram depicted in Figure 3.
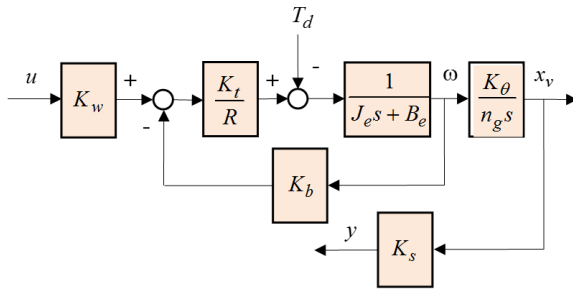

Figure 3. Block diagram of the MOV actuator

When the unknown disturbance is ignored, the transfer function from the control input u to the measured output voltage y is given by

$$G_p(s) = \frac{Y(s)}{U(s)} = \frac{b}{s(s+a)}, \tag{2a}$$

and

$$a = \frac{RB_e + K_t K_b}{RJ_e}, \quad b = \frac{K_w K_t K_\theta K_s}{RJ_e n_g}, \tag{2b}$$

where Ks denotes the sensor gain [V/mm].

3. Nonlinear PD Controller Design

When the position control of the valve stem is considered, the role of the integral action is insignificant due to the inherent integrator from the DC motor (Dessaint et al., 1990). In this study, a NPD controller is considered.

3.1 Controller Structure

The structure of the proposed controller includes a nonlinear gain and the linear PD controller. The nonlinear gain $k(\cdot)$ in cascade with the linear PD controller is a function of the error $e(t)$ between the set-point (or reference input) $r(t)$ and the output $y(t)$ and produces the scaled error $v(t)$ as follows:

$$v(t) = k(e)e(t) = \Phi(e). \tag{3}$$

The linear PD controller is given by

$$u_p(t) = K_p v(t), \tag{4a}$$

$$T_f \dot{u}_d(t) + u_d(t) = K_d \dot{v}(t), \tag{4b}$$

$$u(t) = u_p(t) + u_d(t), \tag{4c}$$

where K_p and K_d are the proportional and derivative gains, respectively, $T_f = K_d/K_p N$ the time constant of the first-order filter, and N an empirically defined constant. N is set to 5 (O'Dwyer, 2006).

The Laplace transform of Equation (4) leads to the transfer function as follows:

$$C(s) = \frac{U(s)}{V(s)} = K_p + \frac{K_d s}{1 + T_f s} \tag{5}$$

3.2 Nonlinear Gain

The proportional term increases or decreases proportionately with the value of e. If a large proportional gain is maintained even for a small error, excessive control can cause overshoot and oscillation. The derivative term also increases or decreases in proportion to the error rate. If a large derivative gain is kept even for a small error, control can be sensitive to noise. Therefore, e should be properly reduced when the response reaches around the set–point. According to this fact, the nonlinear gain is defined by

$$k(e) = k_2 - (k_2 - k_1)\exp(-\frac{e^2}{2\sigma^2}) \tag{6}$$

where k1 and k2 are nonnegative constants (k1<k2) and σ is a parameter. The shape of k(e) depends on the values of k1 and k2 as well as on the value of σ. It is lower bounded by k1 as e=

0 and is upper bounded by k2 as e= ±∞. Figure 4 illustrates the shapes of k(e) versus e for three typical values of σ.
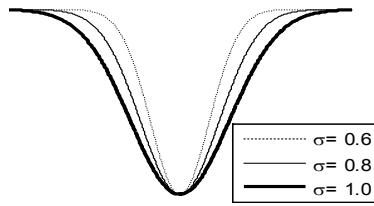

Figure 4. Shapes of $k(e)$ for the typical values of σ

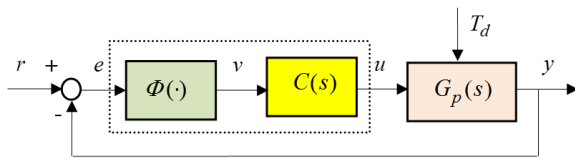Figure 5 depicts the feedback control system with the NPD controller.

Figure 5. NPD control system

3.3 Tuning of the NPD Controller

As shown in Figure 4 and in Equations (3)-(5), the NPD controller has five parameters, K_p, K_d, σ, k_1, and k_2. For convenience, k_1 and k_2 are normalized, $0 \leq k_1 < 1$, and $k_2 = 1$ since a GA optimizes the product of the nonlinear gains and controller gains. Only four parameters K_p, K_d, σ, and k_1 are tuned such that the following objective function is minimized:

$$J = \int_0^\infty |e(t)| + \beta |u(t)| dt,$$ (7)

where β is a weighting factor, which is a user-defined variable.

4. Stability Analysis of the Closed-loop Control System

Since the nonlinear function is used incorporating the PD controller, in this section the stability of the closed-loop system is assessed based on the Popov criterion which is often employed to analyse the stability of nonlinear problems.

Consider a system whose basic structure consists of a linear time-invariant plant $G(s)$ and a nonlinear element Φ. Many systems including the system proposed in Figure 6 can be reduced to this basic form.
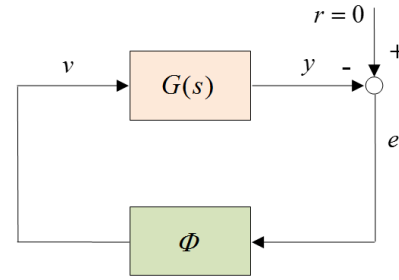

Figure 6. A closed-loop system

Definition 1 (Sector) A memoryless function Φ: $R \rightarrow R$ is said to belong to the sector $[k_1, k_2]$, if there exist two non-negative numbers k_1 and k_2 ($k_1 < k_2$) which can satisfy the following condition:

$$k_1 e \leq \Phi \leq k_2 e, \ \forall e \in R,$$ (8)

where Φ(0)= 0 and for Inequality (8) it is true that $\Phi(e)e = k(e)e^2 \geq 0$ is always satisfied. This fact implies that Φ(e) always lies between the two straight lines $k_1 e$ and $k_2 e$ in the first and third quadrants. Inequality (8) can be simply written as $\Phi \in [k_1, k_2]$.

Figure 7 shows the graphical representation of the sector condition.
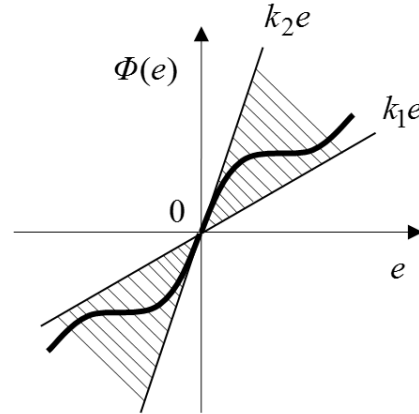

Figure 7. Graphical representation of the sector $[k_1, k_2]$

Theorem 1 (Popov criterion) Consider a closed-loop system as seen in Figure 6, where $G(s)$ has no unstable poles and has no poles on the imaginary axis except for one pole at the origin. Then, the system is absolutely stable if $\Phi \in [0,k]$, $0 < k < \infty$, and there exists a constant q such that the following inequality is satisfied:

$$Re[G(j\omega)] - q\omega Im[G(j\omega)] > -\frac{1}{k},$$

$$\forall \omega \in (-\infty, \infty)$$ (9)

Proof: See Popov (1962) and Khalil (2014) for details.

If the nonlinearity Φ belongs to the sector $[k_1,k_2]$, then it is still possible to use the Popov criterion through the loop transformation in relation to Figure 6.

Applying the loop transformation $\Phi_t(e)= \Phi(e)-k_1 e$ in Figure 8 does not change the interconnection and all the conditions for using the Popov criterion are still satisfied.
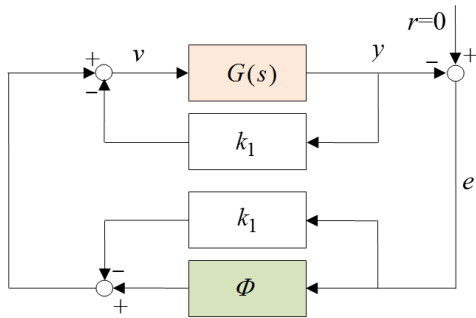

Figure 8. Equivalent closed-loop system

If this transformation is applied, $\Phi \in [k_1,k_2]$ is transformed to $\Phi_t \in [0,k_2-k_1]$, the linear subsystem yields

$$G_t(s) = \frac{G(s)}{1+k_1 G(s)}, \qquad (10)$$

and the Popov inequality in Theorem 1 can be rewritten as

$$Re[G_t(j\omega)] - q\omega Im[G_t(j\omega)] > -\frac{1}{k_2-k_1}, \qquad (11a)$$

or

$$x - qy > -\frac{1}{k_2-k_1}, \qquad (11b)$$

where x is the real part of $G_t(j\omega)$ and y is ω times the imaginary part of $G_t(j\omega)$. If x versus y is plotted, then the condition (11b) is satisfied if the polar plot (Popov plot) lies entirely to the right of the line passing through the point $(-1/k_2-k_1, 0)$ with a slope $1/q$.

If r is assumed to be either 0 or constant when the MOV is operated in regulation mode and T_d is ignored, the system in Figure 5 can be redrawn as shown in Figure 6. Φ belongs to a sector $[k_1,k_2]$, which means that the slope k of Φ is between k_1

and k_2 as shown in Figure 4. The linear block is represented by

$$G(s) = C(s)G_p(s)$$
$$= \frac{b[(K_p T_f + K_d)s + K_p]}{s(s+a)(T_f s+1)}. \qquad (12)$$

Hence, $G_t(s)$ results in

$$G_t(s)$$
$$= \frac{b[(K_p T_f + K_d)s + K_p]}{s(s+a)(T_f s+1) + k_1 b[(K_p T_f + K_d)s + K_p]}. \qquad (13)$$

By substituting the parameter values of the MOV actuator from Table 1 and the controller parameters from Table 2 into Equation (12) it results that $G_t(s)$ has three stable poles, -11.851, -3.182, -1.942. The Popov plot for $\forall \omega > 0$ is depicted in Figure 9. The Popov plot starts at the point $(1/k_1, 0)= (1.253, 0)$ for $\omega= 0$ and ends at the origin $(0, 0)$ for $\omega= \infty$, always stays in the third and fourth quadrant for $\omega > 0$, and never crosses the real axis. It is possible to draw a straight line with a positive slope while passing through $(-1/k_2-k_1, 0)= (-4.95, 0)$ in such a manner that the Popov's plot lies always to the right of the straight line. Thus, the feedback system is absolutely stable.
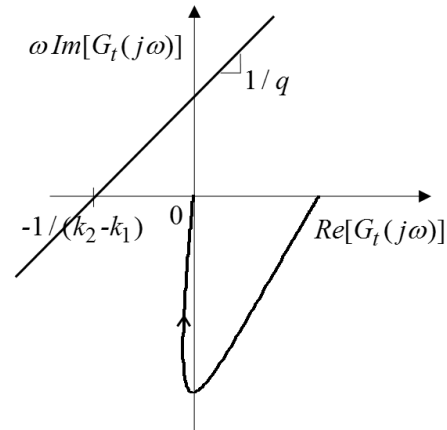

Figure 9. Popov plot of the NPD control system

5. Simulations and Results

A set of simulation works were performed to verify the effectiveness of the proposed NPD controller tuned by a GA. Table 1 shows the parameters of the MOV actuator used in this study.

The performances of the standard PID controller (hereafter referred to as SKO-PID), tuned by using the Skogestad tuning method (Skogestad, 2004), and the SIMULINK PID controller

(hereafter referred to as SIM-PID), which has an automatic tuning scheme, were compared with those of the proposed method. Using the former method, the proportional gain, integral time, and derivative time are $K_p = a/bT_c$, $T_i = \gamma T_c$, and $T_d = 1/a$, respectively. γ was set to 4 by default, and T_c was set to 1.4 by trial and error. Furthermore, the structure of SIM-PID is $C(s) = K_p + K_i/s + K_d s /(1+s/\bar{N})$, and its parameters were automatically tuned.

Table 1. Parameters of the MOV actuator

Parameter	Value
K_w	22
K_t	0.5 [N·m/A]
K_b	0.5 [V·sec]
R	8 [Ω]
J_m	0.0123 [N·m·sec²]
J_L	1 [N·m·sec²]
B_m	0.00588 [N·m·sec]
B_L	0.1 [N·m·sec]
n_g	20
K_θ	0.079 [mm/rad]
K_s	0.439 [V/mm]

The tuning results of the three methods are outlined in Table 2. Meanwhile, $u(t)$ is limited to the minimum u_{min} or the maximum u_{max} when it exceeds the specified linear range due to the physical structure of the valve. u_{min} and u_{max} are set to -10 and 10, respectively. The weighting factor β is set to 0.5.

Table 2. Tuned controller parameters

Method	Gains			Remarks
	K_p	K_i	K_d	
SKO-PID	11.198	1.999	4.434	$T_c = 1.4$, $\gamma = 4$
SIM-PID	8.816	0.911	0.963	$\bar{N} = 0.572$
NPD	39.417	-	13.640	$\sigma = 8.217$, $k_1 = 0.798$

First, an experiment was conducted in which the output follows the set-point (SP) to assess the set-point tracking performance of the proposed controller. At $t = 0$ with the fully closed MOV, SP= 10 [mm], corresponding to the reference input $r = 4.39$ [V], was applied and the valve stem displacements x_v and u were plotted.

Figure 10 and Figure 11 show that all the three methods control with swiftness at the speed of

approximately 75 [mm/min]. It can be noticed that for the SIM-PID and SKO-PID controllers, large overshoots with longer settling times occur. However, the NPD controller shows satisfactory response characteristics. The overshoot occurring when the SP is set to 0 in order to fully close the MOV will trigger the limit switch and/or the torque switch, which shortens the life time of the sensors or the valve seat.
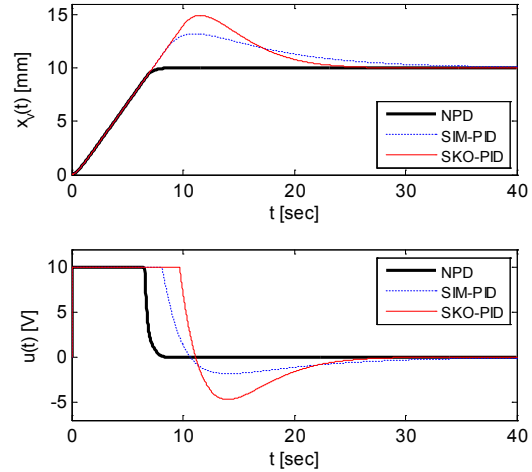

Figure 10. Responses of the three methods when the SP is step-wisely changed from 0 to 10 [mm]
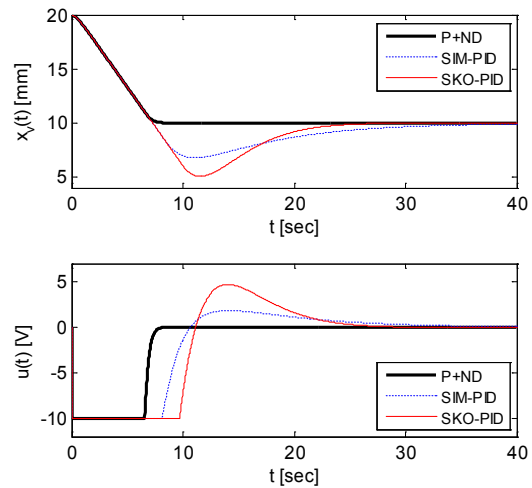

Figure 11. Responses of the three methods when the SP is step-wisely changed from 20 to 10 [mm]

To compare the SP tracking performance of the three methods quantitatively, rise time $t_r = t_{95} - t_5$, peak time t_p, overshoot M_p, 2 [%] settling time t_s, and the sum of the absolute errors (*IAE*) were measured (Table 3). Table 3 shows that the proposed method performs better than the other methods.

Table 3. Quantitative comparison of the SP tracking performances

Method	SP Tracking Performances				
	t_r	t_p	M_p	t_s	*IAE*
NPD	6.340	10.780	0	7.490	38.410
SIM-PID	6.268	11.120	31.994	33.816	75.996
SKO-PID	6.305	6.268	49.248	23.870	76.756

Similarly, the disturbance rejection performance of the proposed method was compared with those of the other methods. For this simulation, a load corresponding to 50 [%] of the rated torque of the motor was applied assuming that disturbance occurs due to the friction between the valve stem and sheet [6]. Figure 12 illustrates the result obtained when a pulse-type load was applied with a size of T_L = 135.5 [N·m] between 5 to 10 [sec] while the SP was kept at 10 [mm] from t= 0.
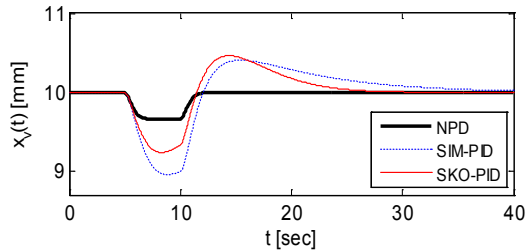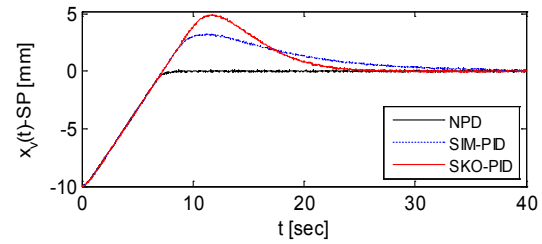
Figure 12. Responses when a pulse-type disturbance is applied

The output of the proposed method was recovered quickly, but those of the other methods were recovered slowly with longer settling time due to the effect of the disturbance.

Finally, a simulation was performed to verify the robustness of the proposed method for noises from the sensor. A Gaussian noise, $N(0, 0.015^2)$ was applied to the feedback signal, where 3σ corresponds to approximately 1 [%] of the SP, and (x_v–SP) was plotted so that the effect of noise would be enlarged.

Figure 13. Responses of (x_v–SP) when Gaussian noise $N(0, 0.015^2)$ is applied

As seen in Figure 13, the output of the proposed method stayed close to the SP, despite the noises, but the SIM-PID generated a little offset due to the noises.

6. Conclusion

As a preliminary stage of developing a MOV, its mathematical models were derived and a nonlinear PD controller incorporating a simple nonlinear function was proposed. The proposed controller was tuned using a GA in order to minimize the objective function. The stability assessment of the closed-loop system was evaluated by applying the Popov stability criterion and its graphical interpretation.

Moreover, the SP tracking performance, the disturbance rejection performance, and the robustness to noise of the three different controllers were compared. From the simulation results, it was found that the proposed method showed better performances in comparison with the other two methods.

Acknowledgements

REFERENCES

1. Ali, M. M. & Al-Khawaldeh, A. (2016). A Simulation Study of Multi-Disciplinary Position Control Methods of Robot Arm DC Motor. In *Proceedings of the 2016 13th International Multi-Conference on Systems, Signals & Devices* (pp. 489-493).

2. Cheng, G. (1997). *Genetic Algorithm & Engineering Design*. John Wiley & Sons, Inc.

3. Dessaint, L. A., Hebert, B. J., Le-Huy, H. & Cavuoti, G. (1990). A DSP-Based Adaptive Controller for a Smooth Positioning System, *IEEE Transactions on Industrial Electronics*, *37*(5), 372-377.

4. EPRI (1990). *Application Guide for Motor Operated Valves in Nuclear Power Plants*, *9*, NP-6660-D.

5. Hussain, B. H., Behera, K. & Alsammarae, A. J. (1996). Study of MOV Operator and Motor Characteristics to Determine Torque Capability, *IEEE Transactions on Nuclear Science*, *42*(6), 2271-2274.

6. Jung, K., Kim B. & Lee H. (2004). Development of a diagnostic system for MOVs, *Mechanics and Materials*, 67-81.

7. Jung, J. & Seong, P. (2003). Error Analysis in Improved Motor Control Center Method for Stem Thrust Estimation of Motor-Operated Valves in Nuclear Power Plants, *IEEE Transactions on Nuclear Science*, *50*(3), 735-740.

8. Kang, S. et al. (2011). A Study on the Stem Friction Coefficient Behaviour of Motor-Operated Valves, *Nuclear Engineering and Design*, *241*(3), 961-967.

9. Khalil, H. K. (2014). *Nonlinear Systems*, 3rd Edition. Pearson Education Limited, Britain.

10. Limitorque (2019). <https://www.flowserve.com/en/limitourque>.

11. Ministry of Science and Technology (1997). *Regulatory Documents for Motor-Operated Valve (MOV) and MOV Gate Valves*, 71233-205.

12. O'Dwyer, A. (2006). *Handbook of PI and PID Controller Tuning Rules*, 2nd Edition. Imperial College Press, Britain, 978-1-78326-004-1.

13. Owayjan, M, Daou, R. A. Z. & Moreau, X. (2015). A Comparison between Frequency Domain and Time Domain Controller Synthesis: Position Control of a DC Motor. In *Proceedings of the 2015 Third International Conference on Technological Advances in Electrical, Electronics and Computer Engineering (TAEECE)* (pp. 201-206).

14. Popov, V. M. (1962). Absolute Stability of Nonlinear Systems of Automatic Control, *Automation and Remote Control*, *22*(8), 857-875.

15. Skogestad, S. (2004). Simple analytic rules for model reduction and PID controller tuning, *Modeling, Identification and Control*, *25*(2), 85-120.

16. United States Nuclear Regulatory Commission (1989). Safety-Related (1) Motor-Operated Valve Testing and Surveillance Results of the Public Workshops, *Generic Letter No. 89-10*, <https://www.nrc.gov/reading-rm/doc-collections/gen-comm/gen-letters/1989 / gl89010.html>.

17. Wadhwani, S. & Verma, V. (2013). Evolutionary Computation Techniques Based Optimal PID Controller Tuning, *International Journal of Engineering Trends and Technology*, *4*(6), 2529-2534.